

# Microstructure Evolution of Gold-Tin Eutectic Solder on Cu and Ni Substrates

J.Y. TSAI,<sup>1</sup> C.W. CHANG,<sup>1</sup> C.E. HO,<sup>1</sup> Y.L. LIN,<sup>1</sup> and C.R. KAO<sup>1-3</sup>

1.—Department of Chemical & Materials Engineering, National Central University, Chungli City, Taiwan. 2.— Institute of Materials Science & Engineering, National Central University. 3.—E-mail: kaocr@hotmail.com

The microstructures of the eutectic Au<sub>20</sub>Sn (wt.%) solder that developed on the Cu and Ni substrates were studied. The Sn/Au/Ni sandwich structure (2.5/3.75/2 μm) and the Sn/Au/Ni sandwich structure (1.83/2.74/5.8 μm) were deposited on Si wafers first. The overall composition of the Au and the Sn layers in these sandwich structures corresponded to the Au<sub>20</sub>Sn binary eutectic. The microstructures of the Au<sub>20</sub>Sn solder on the Cu and Ni substrates could be controlled by using different bonding conditions. When the bonding condition was 290°C for 2 min, the microstructure of Au<sub>20</sub>Sn/Cu and Au<sub>20</sub>Sn/Ni was a two-phase (Au<sub>5</sub>Sn and AuSn) eutectic microstructure. When the bonding condition was 240°C for 2 min, the AuSn/Au<sub>5</sub>Sn/Cu and AuSn/Au<sub>5</sub>Sn/Ni layered microstructure formed. After bonding, the Au<sub>20</sub>Sn/Cu and Au<sub>20</sub>Sn/Ni diffusion couples were subjected to aging at 240°C. The thermal stability of Au<sub>20</sub>Sn/Ni was better than that of Au<sub>20</sub>Sn/Cu. Moreover, less Ni was consumed compared to that of Cu. This indicates that Ni is a more effective diffusion barrier material for the Au<sub>20</sub>Sn solder.

**Key words:** Au-Sn, diffusion couple, lead-free solder

## INTRODUCTION

The 80Au<sub>20</sub>Sn (wt.%, Au<sub>20</sub>Sn) solder is an important bonding material for the packaging of optoelectronic devices because of its many attractive properties. First, this solder becomes molten at a relatively low eutectic temperature of 278°C. Second, its relatively high yield strength makes it more resistant to creep. Consequently, Au<sub>20</sub>Sn is useful for bonding devices that are sensitive to high processing temperatures but need good creep resistance. Such applications include the bonding of GaAs<sup>1-3</sup> or large Si dies<sup>4</sup> on alumina. Moreover, the bonding processes using Au<sub>20</sub>Sn can be fluxless due to its high Au content. Last, the high thermal conductivity of Au<sub>20</sub>Sn (57 W/m°C) makes it particularly useful for bonding higher power devices that demand good heat dissipation.

According to the Au-Sn binary phase diagram,<sup>5</sup> the Au<sub>20</sub>Sn alloy at the solid state has Au<sub>5</sub>Sn and AuSn as its constituents. The Au<sub>5</sub>Sn phase has two stable forms, the low temperature ordered phase ζ',

which is a line compound at 16.0 at.% Sn, and the high-temperature disordered phase ζ, which has a homogeneity range of 9.1–17.6 at.% Sn. The AuSn phase has the NiAs-type hexagonal structure with a homogeneous range between 50.0 at.% and 50.5 at.% Sn, and melts congruently at 419.3°C.

In optoelectronic packaging applications, Ni and Cu are two of the most common metals to be in direct contact with the solders. They are often used as the top surface finish metals on the soldering pads of the devices or the substrates. The reactions of the solders and the surface finish metals are important because the interfaces often control the overall strength of the solders joints. The reaction of the Sn/Au/Ni sandwich structure has been studied before.<sup>6</sup> It was found that this reaction was quite complicated but at the same time quite interesting. It was shown that the microstructures of Au<sub>20</sub>Sn on Ni could be controlled by different bonding conditions.<sup>6</sup> When the bonding condition was 290°C for 2 min, the microstructure produced was a typical two-phase (Au<sub>5</sub>Sn and AuSn) eutectic microstructure over Ni. In contrast, when the bonding condition was 240°C for 2 min, an AuSn/Au<sub>5</sub>Sn/Ni layered micro-

structure was produced. When this AuSn/Au<sub>5</sub>Sn/Ni layered structure was subjected to aging at 240°C, the AuSn layer gradually exchanged its position with the Au<sub>5</sub>Sn layer, and formed a Au<sub>5</sub>Sn/AuSn/Ni layered structure in less than 9 h. The dominant diffusing species in the AuSn and Au<sub>5</sub>Sn phases has also been identified to be Au and Sn, respectively. The objective of this study is to study the reaction of the Au20Sn solder and the other common surface finish metal Cu. The difference between the Sn/Au/Ni reaction and the Sn/Au/Cu reaction will also be compared with the eventual purpose of identifying a better surface finish metal for the Au20Sn solder.

### EXPERIMENTAL

The samples used in this study were formed by depositing the Sn/Au/Ni or Sn/Au/Cu three-layer sandwich structure onto Si wafers through evaporation. For the Sn/Au/Ni samples, the thickness of Sn, Au, and Ni was 2.5 μm, 3.75 μm, and 2.0 μm, respectively. For the Sn/Au/Cu samples, the thickness of Sn, Au, and Cu was 1.83 μm, 2.74 μm, and 5.8 μm, respectively. The amounts of Au and Sn in these two types of samples, if uniformly mixed, will produce an alloy with the Au20Sn composition.

The samples were first bonded for 2 min either at 240°C or at 290°C. This short processing time at 240°C or 290°C was long enough for the Au layer and the Sn layer to react to produce a Au20Sn alloy over the Ni or Cu substrates, forming the Au20Sn/Ni or the Au20Sn/Cu diffusion couples. Then, the Au20Sn/Ni and Au20Sn/Cu diffusion couples were aged at 240°C for up to 1000 h. Subsequently, the samples were mounted in epoxy and metallurgically polished in preparation for characterization. The reaction zone for each sample was examined using a scanning electron microscope (SEM). The compositions of each phase were determined using a JEOL JXA-8800M electron microprobe (Japan Electron Optics Ltd., Tokyo), operated at 20 keV. In microprobe analysis, the concentration of each element was measured independently, and the total weight percentage of all elements was within 100 ± 1% in each case. The average value from at least three measurements was then reported. For the x-ray diffraction (XRD) analysis, the Cu K<sub>α</sub> radiation was used.

### RESULTS

In the following, the microstructure evolution during bonding at 290°C or 240°C for two min to form Au20Sn/Ni and Au20Sn/Cu is presented first. Then the results from the aging of Au20Sn/Ni and Au20Sn/Cu at 240°C are presented.

#### Bonding Reaction at 290°C or 240°C for 2 Min

As mentioned earlier, the microstructure of Au20Sn on Ni could be controlled by the bonding conditions of the Sn/Au/Ni sandwich. When the bonding condition was at 290°C for 2 min, the microstructure of (Au, Ni)<sub>5</sub>Sn and (Au, Ni)Sn was a

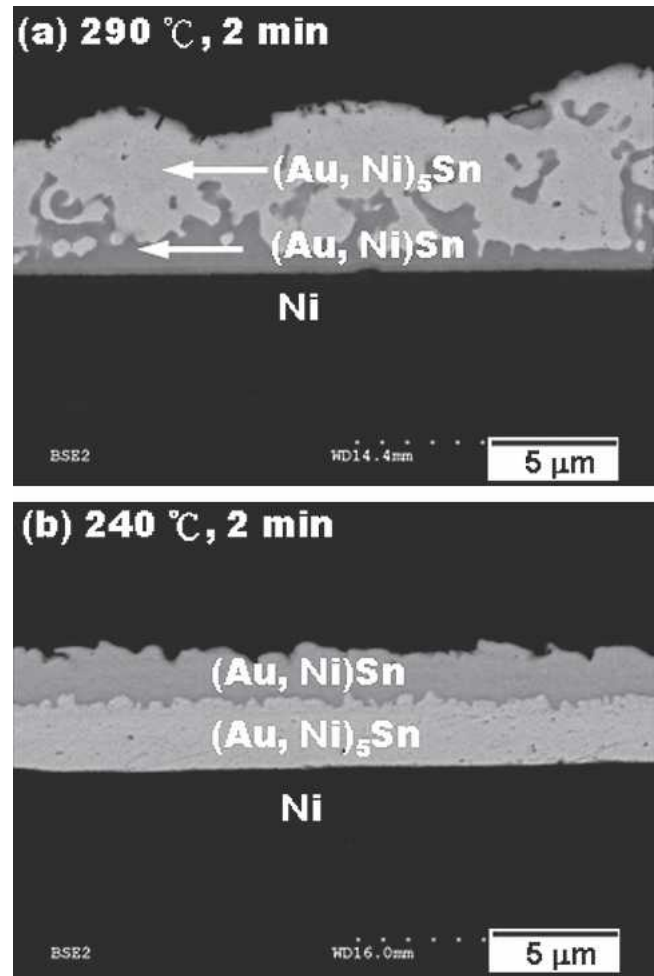


Fig. 1. Microstructures of Sn/Au/Ni after bonding for 2 min at (a) 290°C and (b) 240°C. The reaction products were (Au, Ni)<sub>5</sub>Sn and (Au, Ni)Sn in both cases, but had different morphologies. An eutectic microstructure formed at 290°C, and a layered microstructure formed at 240°C.

eutectic type, as shown in Fig. 1a. When the bonding condition was at 240°C for 2 min, both (Au, Ni)<sub>5</sub>Sn and (Au, Ni)Sn has a layered morphology, as shown in Fig. 1b. The phase sequence was also different for these two cases. At 290°C, (Au, Ni)Sn was next to the Ni phase, while (Au, Ni)<sub>5</sub>Sn was next to the Ni phase at 240°C.

This sensitivity of the microstructure to the bonding conditions also exists for the Sn/Au/Cu samples. Figure 2a shows the microstructure of Sn/Au/Cu after bonding at 290°C for 2 min. The two reaction products formed over Cu were (Au, Cu)<sub>5</sub>Sn and (Au, Cu)Sn, according to the electron-probe microanalysis (EPMA) measurements. These two compounds have Au<sub>5</sub>Sn and AuSn crystal structures, respectively, but have small amounts of Cu dissolved in the Au sublattices. From the EPMA measurements, the concentration of Cu was 2.5 at.% in (Au, Cu)Sn and 17 at.% in (Au, Cu)<sub>5</sub>Sn. Consequently, these two phases here can be labeled as (Au<sub>0.95</sub>Cu<sub>0.05</sub>)Sn and (Au<sub>0.80</sub>Cu<sub>0.20</sub>)<sub>5</sub>Sn, respectively. The (Au, Cu)<sub>5</sub>Sn phase was a continuous layer, but the (Au, Cu)Sn phase was discontinuous. In contrast, bonding at

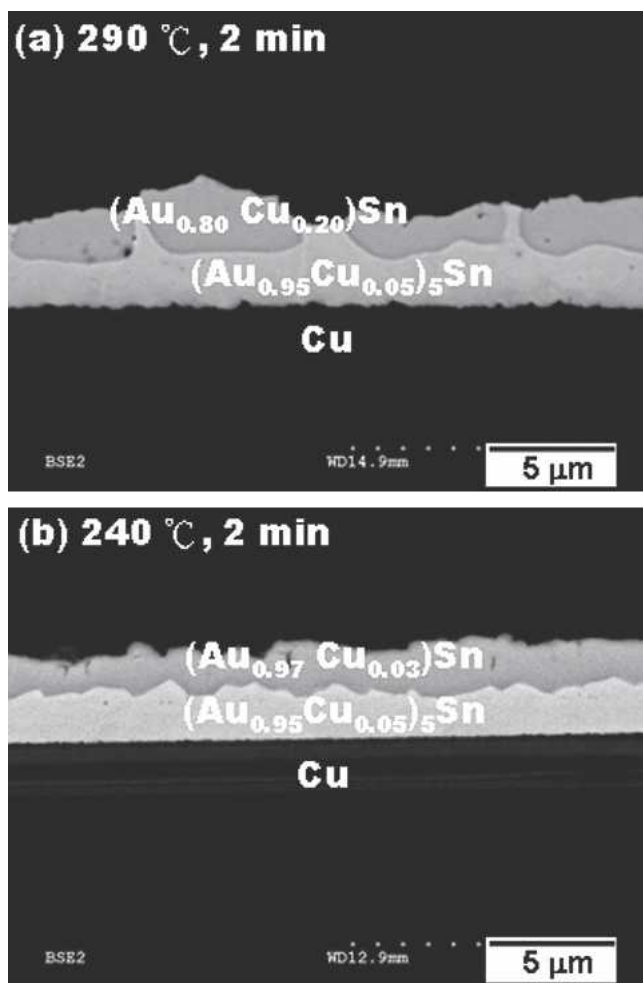


Fig. 2. Microstructures of Sn/Au/Cu after bonding for 2 min at (a) 290°C and (b) 240°C. The reaction products were  $(\text{Au}, \text{Cu})_5\text{Sn}$  and  $(\text{Au}, \text{Cu})\text{Sn}$  in both cases, but had different morphologies. The  $(\text{Au}, \text{Cu})\text{Sn}$  phase was discontinuous at 290°C, but was a continuous layer at 240°C.

240°C for 2 min produced two continuous layers,  $(\text{Au}, \text{Cu})_5\text{Sn}$  and  $(\text{Au}, \text{Cu})\text{Sn}$ , as shown in Fig. 2b. From the EPMA measurements, the concentration of Cu was 1.5 at.% in  $(\text{Au}, \text{Cu})\text{Sn}$  and 4.3 at.% in  $(\text{Au}, \text{Cu})_5\text{Sn}$ . Therefore, these two phases here can be labeled as  $(\text{Au}_{0.97}\text{Cu}_{0.03})\text{Sn}$  and  $(\text{Au}_{0.95}\text{Cu}_{0.05})_5\text{Sn}$ , respectively. As expected, the Cu concentrations were lower in  $(\text{Au}, \text{Cu})\text{Sn}$  and  $(\text{Au}, \text{Cu})_5\text{Sn}$  when the bonding was done at a lower temperature. It should be noted that here the phase sequence was the same for the two conditions used. The phase  $(\text{Au}, \text{Cu})_5\text{Sn}$  always formed next to Ni.

#### Aging Reaction at 240°C

The results from the Sn/Au/Cu samples that were bonded at 290°C for 2 min, followed by aging at 240°C, are presented first. Figure 3a shows what happened when the microstructure in Fig. 2a was aged at 240°C for 1 h. The overall microstructure and the phases present did not change, but the concentrations of Cu in  $(\text{Au}, \text{Cu})\text{Sn}$  and  $(\text{Au}, \text{Cu})_5\text{Sn}$  increased. According to detailed EPMA,  $(\text{Au}, \text{Cu})_5\text{Sn}$

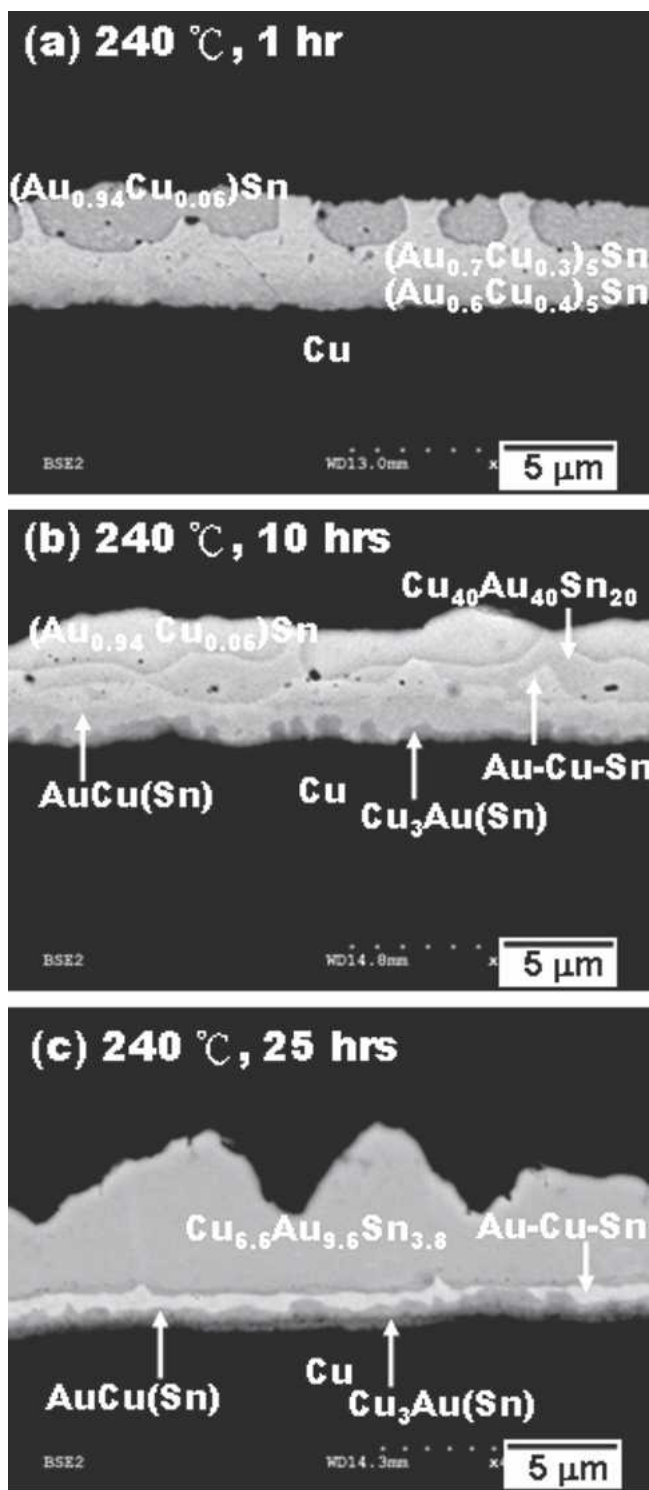


Fig. 3. Backscattered electron micrographs showing the microstructures of Au<sub>20</sub>Sn/Cu that has been reacted at 290°C for 2 min, followed by aging at 240°C for (a) 1 h, (b) 10 h, and (c) 25 h.

in fact has two distinct composition ranges,  $(\text{Au}_{0.7}\text{Cu}_{0.3})_5\text{Sn}$  and  $(\text{Au}_{0.6}\text{Cu}_{0.4})_5\text{Sn}$ , as labeled in Fig. 3a. This implies that the  $\text{Au}_5\text{Sn}$  phase can dissolve a substantial amount of Cu at 240°C. According to the Au-Cu-Sn isotherm at 190°C (Fig. 4), determined by Zakeł,<sup>7</sup>  $\text{Au}_5\text{Sn}$  indeed has a high Cu solubility (19 at.% Cu) at 190°C. When the reaction

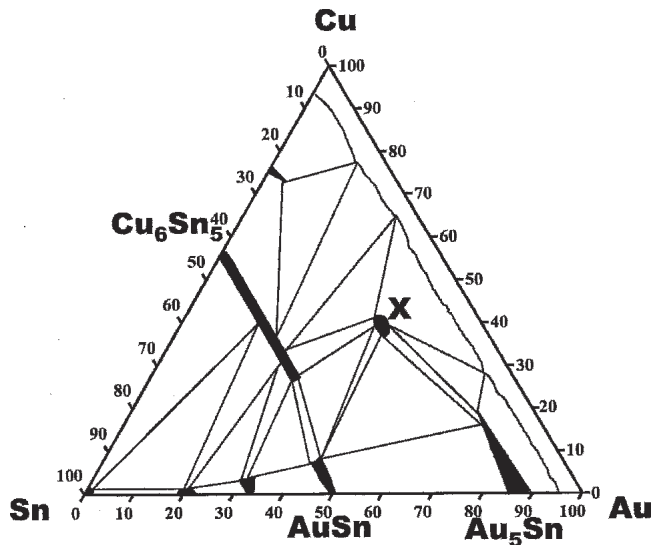


Fig. 4. The Au-Cu-Sn ternary isotherm at 190°C. This isotherm was determined by Zakei.<sup>7</sup>

time reached 10 h, the microstructure became very complicated, as shown in Fig. 3b. The composition of (Au, Cu)Sn remained  $(\text{Au}_{0.94}\text{Cu}_{0.06})\text{Sn}$ . In addition, there were a  $\text{Cu}_{40}\text{Au}_{40}\text{Sn}_{20}$  phase, an Au-Cu-Sn ternary compound with unknown composition, an AuCu phase with a small amount of Sn dissolved, and a  $\text{Cu}_3\text{Au}$  phase with a small amount of Sn dissolved. The composition of the Au-Cu-Sn ternary compound as well as the Sn contents in AuCu and  $\text{Cu}_3\text{Au}$  could not be measured accurately because these phases were too small for accurate EPMA. When the reaction time reached 25 h (Fig. 3c), the composition of the outer layer was  $\text{Au}_{35}\text{Cu}_{47}\text{Sn}_{18}$  according to the EPMA measurement. According to the x-ray diffraction analysis shown in Fig. 5, this compound was based on the  $\text{Au}_{6.6}\text{Cu}_{9.6}\text{Sn}_{3.8}$  structure. This compound  $\text{Au}_{6.6}\text{Cu}_{9.6}\text{Sn}_{3.8}$  was not in the Au-Cu-Sn isotherm shown in Fig. 4, but has been identified and indexed in the literature.<sup>8</sup> In addi-

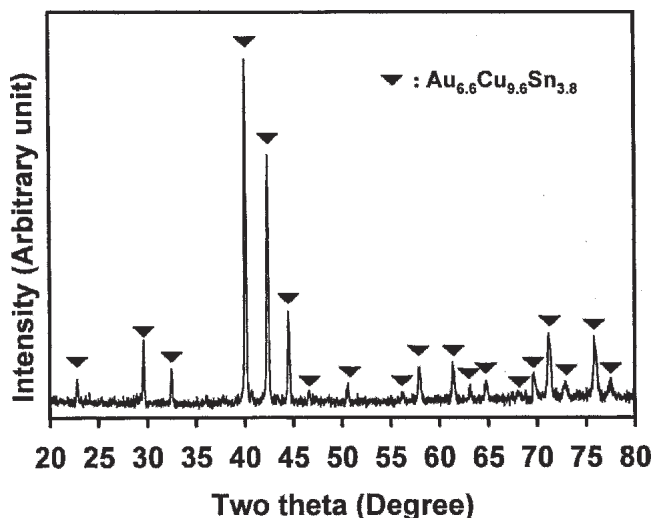


Fig. 5. X-ray diffraction pattern of the  $\text{Au}_{6.6}\text{Cu}_{9.6}\text{Sn}_{3.8}$  phase. The  $\text{Cu K}\alpha_1$  radiation was used.

tion, there were an Au-Cu-Sn ternary compound, a  $\text{CuAu}(\text{Sn})$  phase, and a  $\text{Cu}_3\text{Au}(\text{Sn})$  phase. Again, the exact compositions could not be determined accurately.

As shown in Fig. 6, the aging behavior of those Sn/Au/Cu samples that were bonded at 240°C for 2 min was very similar to those that were bonded at

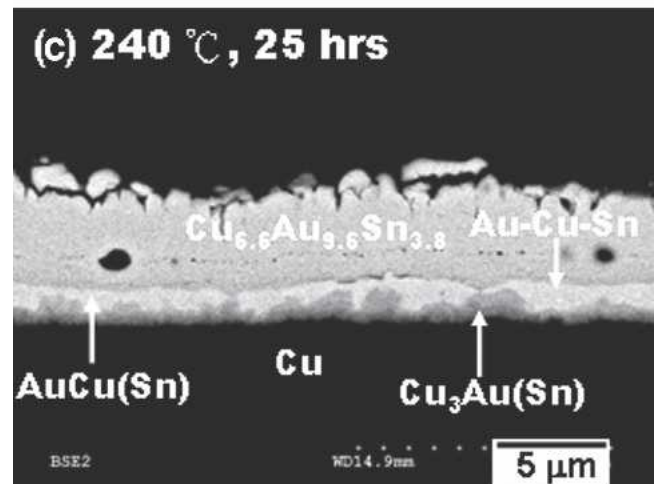
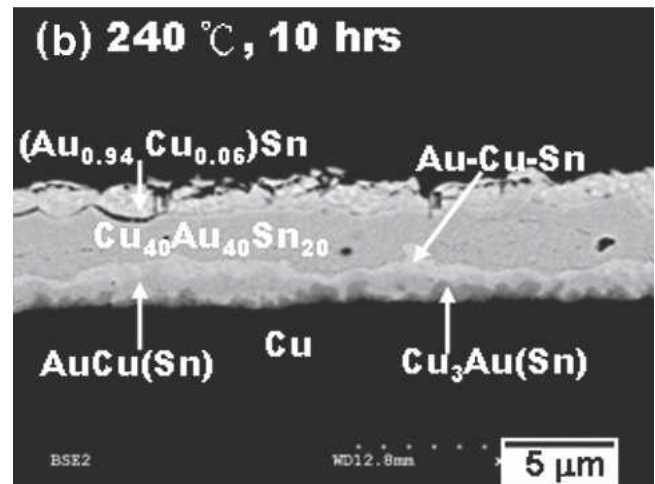
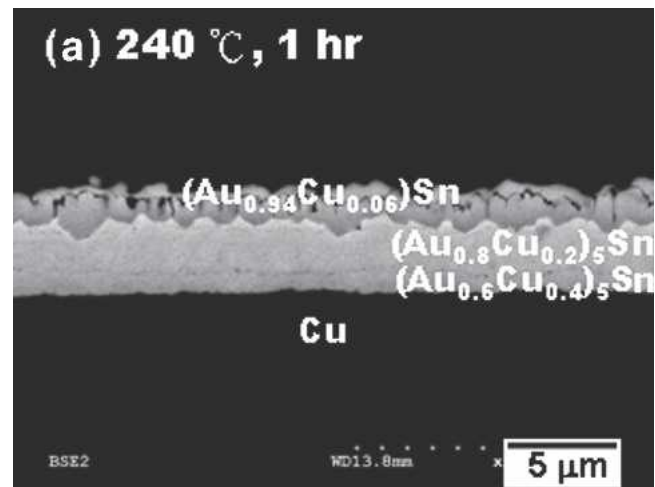


Fig. 6. Backscattered electron micrographs showing the microstructures of Au20Sn/Cu that were reacted at 240°C for 2 min, followed by aging at 240°C for (a) 1 h, (b) 10 h, and (c) 25 h.

290°C. In other words, the initial difference induced during bonding disappeared rather quickly.

The reaction between Au<sub>20</sub>Sn and Ni at 240°C was less extensive compared to that between Au<sub>20</sub>Sn and Cu presented above. As has been pointed out in a previous study,<sup>6</sup> when the microstructure in Fig. 1b was aged at 240°C, (Au, Ni)Sn and (Au, Ni)<sub>5</sub>Sn exchanged their positions. Figure 7 is an example of (Au, Ni)Sn and (Au, Ni)<sub>5</sub>Sn after they have finished exchanging their positions. It seemed that (Au, Ni)Sn preferred to have Ni as its immediate neighbor. It should be noted that (Au, Ni)Sn was next to Ni right after bonding when the bonding was carried out at 290°C. The observation that higher bonding temperature and longer aging time both made (Au, Ni)Sn preferentially locate next to Ni seems to suggest that the reason for this preference is thermodynamic in nature. In addition to (Au, Ni)Sn and (Au, Ni)<sub>5</sub>Sn, a thin intermetallic compound layer between (Au, Ni)Sn and Ni formed after 208 h of aging. According to EPMA measurement, this compound was an Au-Ni-Sn ternary compound, and was probably the Ni<sub>3</sub>Sn<sub>2</sub> phase with a large amount of Au dissolved.<sup>6</sup>

Figure 8 shows the microstructures of Au<sub>20</sub>Sn/Ni and Au<sub>20</sub>Sn/Cu that were aged at 240°C for 1000 h. It is clear that the microstructure of Au<sub>20</sub>Sn on Ni was more thermally stable than on Cu. As shown in Fig. 8a, the microstructure of Au<sub>20</sub>Sn/Ni remained layered after aging at 240°C for 1000 h. The composition of the upper layer became Au<sub>88.1</sub>Ni<sub>0.9</sub>Sn<sub>11</sub>. According to the x-ray diffraction result shown in Fig. 9, this layer was still (Au, Ni)<sub>5</sub>Sn. The (Au, Ni)Sn layer, which still existed after 208 h of aging (Figure 7), disappeared. The thick layer under the (Au, Ni)<sub>5</sub>Sn layer has the composition Au<sub>23</sub>Ni<sub>35</sub>Sn<sub>42</sub>. From the x-ray diffraction analysis shown in Fig. 10, this compound was identified to be the Ni<sub>3</sub>Sn<sub>2</sub> phase with a large amount of Au dissolved. Between Ni and (Ni<sub>0.6</sub>Au<sub>0.4</sub>)<sub>3</sub>Sn<sub>2</sub>, there was a darker Au-Ni-Sn ternary compound, which remained unidentified.

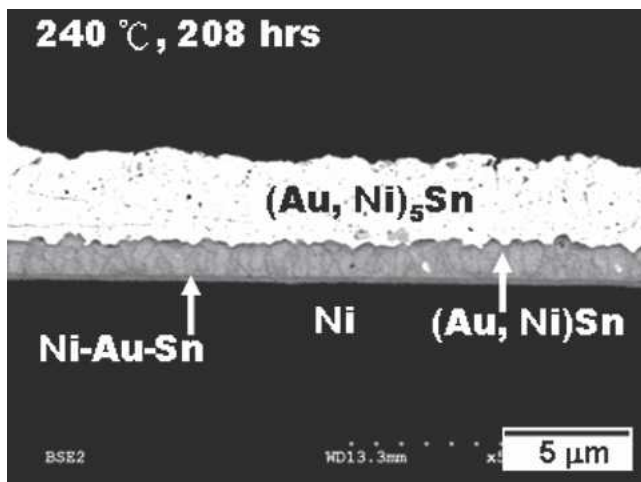


Fig. 7. Backscattered electron micrographs showing the microstructure of Sn/Au/Ni that were bonded at 240°C for 2 min, followed by aging at 240°C for 208 h.

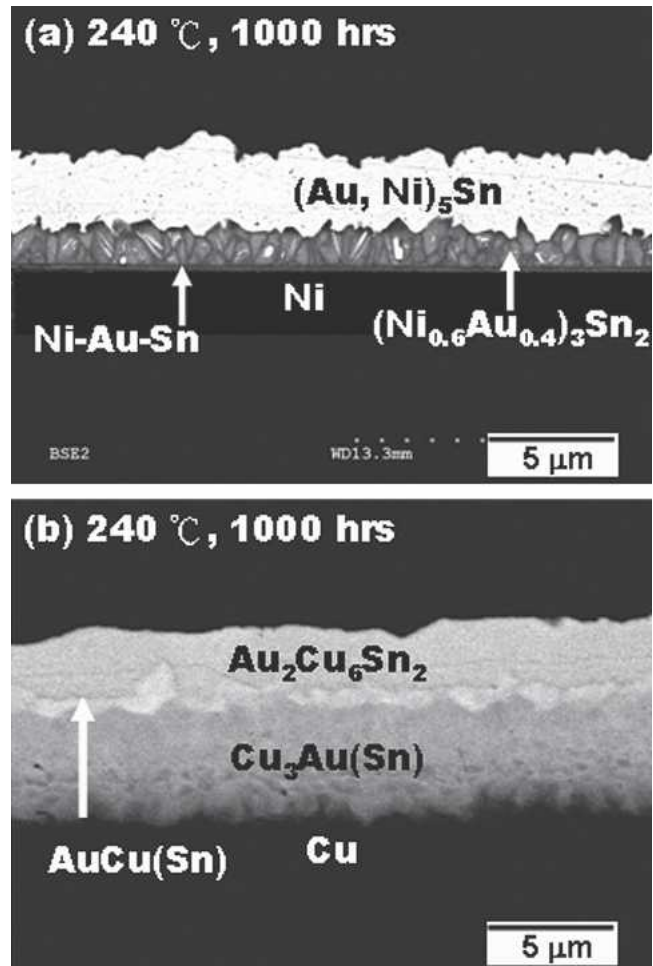


Fig. 8. Backscattered electron micrographs showing the microstructure of (a) Au<sub>20</sub>Sn/Ni and (b) Au<sub>20</sub>Sn/Cu that has been aged at 240°C for 1000 h.

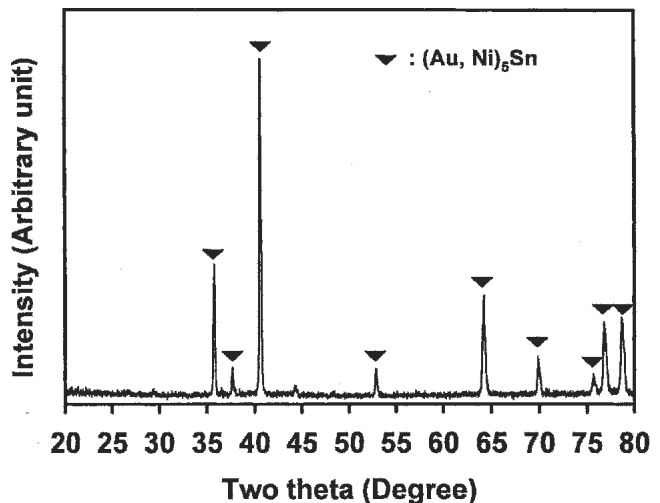


Fig. 9. X-ray diffraction pattern for the upper layer of the sample shown in Fig. 8a. The phase is identified to be (Au, Ni)<sub>5</sub>Sn. The Cu K $\alpha_1$  radiation was used.

The consumed thickness of Ni after aging at 240°C for 1000 h was 0.8  $\mu$ m regardless of the bonding condition.

Figure 8b shows the microstructures of Au<sub>20</sub>Sn/

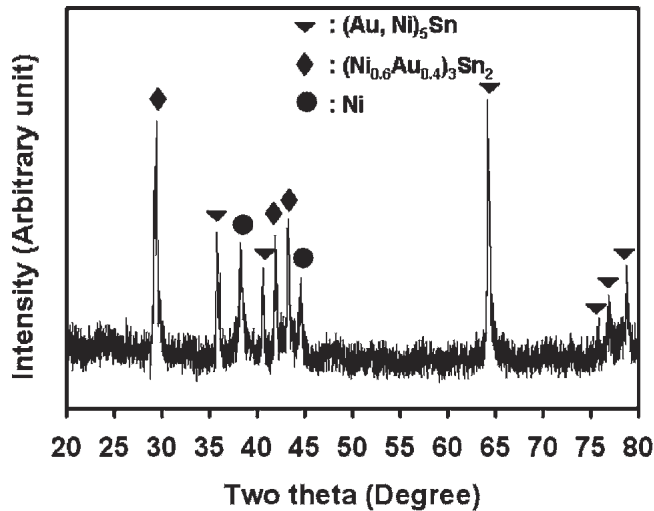


Fig. 10. X-ray diffraction pattern for the second layer of the sample shown in Fig. 8a. Most of the upper layer has been removed by etching. The  $\text{Cu K}\alpha_1$  radiation was used.

Cu that was aged at  $240^\circ\text{C}$  for 1000 h. The upper layer became  $\text{Au}_2\text{Cu}_6\text{Sn}_2$  according to the x-ray diffraction analysis (Fig. 11). The  $\text{Au}_2\text{Cu}_6\text{Sn}_2$  phase was not in the Au-Cu-Sn isotherm shown in Fig. 4, but its existence and crystal structure have been established in the literature.<sup>9</sup> The consumed thickness of Cu now was  $4.8\ \mu\text{m}$ , much greater than that of Ni.

### DISCUSSION

There are several differences between the Sn/Au/Ni or Sn/Au/Cu diffusion couples. During the bonding,  $\text{Au}_5\text{Sn}$  preferred to form next to Cu in both bonding conditions, as shown in Fig. 2, and AuSn preferred to form next to Ni, as shown in Fig. 1a. It should be noted that, even though  $\text{Au}_5\text{Sn}$  initially formed next to Ni when the bonding temperature was at  $240^\circ\text{C}$ , as shown in Fig. 1b,  $\text{Au}_5\text{Sn}$  and AuSn exchanged their positions during aging and the AuSn phase eventually was next to Ni, as shown in Fig. 7. In other words, before extensive interactions

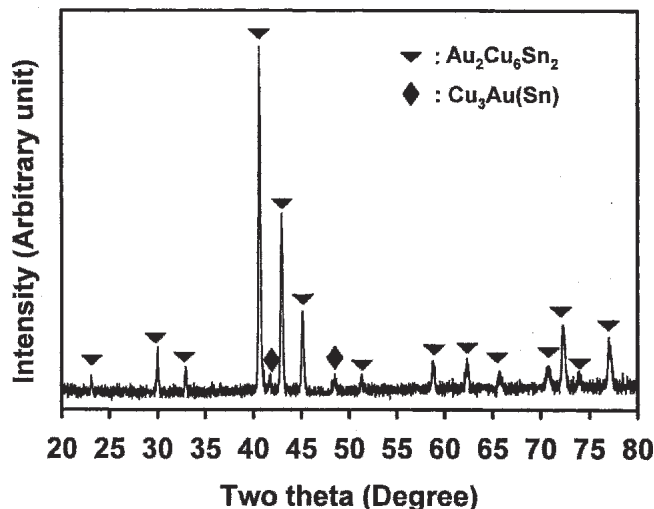


Fig. 11. X-ray diffraction pattern for the sample in Fig. 8b. The  $\text{Cu K}\alpha_1$  radiation was used.

between  $\text{Au}_{20}\text{Sn}$  and Ni or Cu, the  $\text{Au}_5\text{Sn}$  phase in  $\text{Au}_{20}\text{Sn}$  has a tendency to be next to Cu, and the AuSn phase has a tendency to be next to Ni. This observation indicates that the selection of the contact materials can influence the microstructures of the  $\text{Au}_{20}\text{Sn}$ . The reason that Cu and Ni have different affinities toward  $\text{Au}_5\text{Sn}$  and AuSn is not clear at present. According to the Au-Cu-Sn isotherm shown in Fig. 4, there are tie-lines between  $\text{Au}_5\text{Sn}$  and the Au-Cu solid solution, but there is no tie-line between the AuSn and the Au-Cu phases. Therefore, the affinity between  $\text{Au}_5\text{Sn}$  and Cu can be rationalized with this thermodynamic argument. However, this type of argument cannot be applied to explain the affinity between AuSn and Ni, as neither AuSn nor  $\text{Au}_5\text{Sn}$  is in thermodynamic equilibrium with Ni according to the Au-Ni-Sn isotherm shown in Fig. 12. Consequently, for the Ni case we can only say that the system simply chooses that particular diffusion path.

The results of this study also show that the thermal stability of  $\text{Au}_{20}\text{Sn}/\text{Ni}$  was better than that of  $\text{Au}_{20}\text{Sn}/\text{Cu}$  when these diffusion couples were subjected to long-term aging at  $240^\circ\text{C}$ . However, even for the  $\text{Au}_{20}\text{Sn}/\text{Ni}$  couple, the (Au, Ni)Sn/Ni interface in Fig. 1 or 7 was not in thermodynamic equilibrium according to the Au-Ni-Sn isotherm shown in Fig. 12.<sup>10</sup> Considering a diffusion couple between Ni and the (Au, Ni)Sn phase, there is no tie-line connecting these two phases. Therefore, the (Au, Ni)Sn/Ni interface was not in thermodynamic equilibrium. It follows that there was a driving force for a new phase to form at the (Au, Ni)Sn/Ni interface. According to the isotherm, the  $(\text{Ni, Au})_3\text{Sn}_2$  phase has a good chance to form at the interface because of the fact that there is a tie-line between Ni and  $(\text{Ni, Au})_3\text{Sn}_2$  as well as between  $(\text{Ni, Au})_3\text{Sn}_2$  and (Au, Ni)Sn. For the  $\text{Au}_{20}\text{Sn}/\text{Ni}$  diffusion couple, aging at  $240^\circ\text{C}$  for 1000 h made the (Au, Ni)Sn phase disappear and induced the formation of  $(\text{Ni, Au})_3\text{Sn}_2$  and

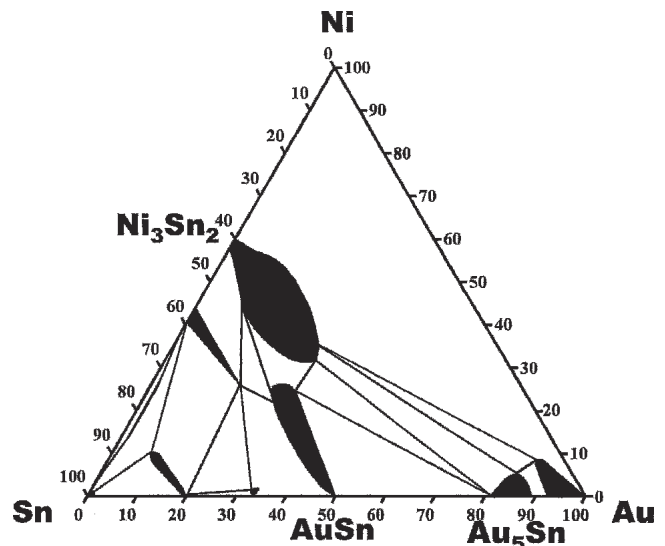


Fig. 12. The Au-Ni-Sn ternary isotherm at room temperature. This isotherm was determined by Anhöck et al.<sup>10</sup>

a ternary compound Au-Ni-Sn. Considering the initial thickness of the Au layer (3.75  $\mu\text{m}$ ), that of the Sn layer (2.5  $\mu\text{m}$ ), and the consumed thickness of the Ni layer (0.8  $\mu\text{m}$ ), one can calculate that the overall composition is  $\text{Au}_{57.2}\text{Ni}_{18.9}\text{Sn}_{23.9}$ . This composition is in the  $\text{Au}_5\text{Sn} + \text{Ni}_3\text{Sn}_2$  two-phase field according to the Au-Ni-Sn isotherm shown in Fig. 12. This explains the coexistence of these two phases in the Au20Sn couple after 1000 h of aging. The new Au-Ni-Sn ternary compound could be the  $\text{Ni}_3\text{Sn}$  phase with a small amount of Au dissolved.

The evolution of the Au20Sn/Cu was much faster and more complicated. It has been reported that Cu was the most mobile species in the Au-Cu-Sn system.<sup>11</sup> Therefore, Cu could diffuse into Au20Sn solder easily, and consequently, the Au-Sn compounds were replaced by Au-Cu-Sn and Au-Cu compounds. There were two compounds formed in the Au20Sn/Cu couple,  $\text{Au}_{6.6}\text{Cu}_{9.6}\text{Sn}_{3.8}$  and  $\text{Au}_2\text{Cu}_6\text{Sn}_2$ , which were not included in the Au-Cu-Sn 190°C phase diagram.<sup>7</sup> Nevertheless, the existence of these two compounds has been reported in the literature.<sup>8,9</sup> Therefore, the Au-Cu-Sn phase diagram at 240°C needs to be studied in more detail in the future.

### CONCLUSIONS

The microstructures of the Au20Sn solder on Cu and Ni substrates can be controlled by reacting Au and Sn at different conditions. When the reaction condition was 290°C for 2 min, the microstructure was a eutectic type, which was a mixture of  $\text{Au}_5\text{Sn}$  and AuSn. The major difference between Au20Sn/Ni and Au20Sn/Cu was that (Au, Ni)Sn preferred to form next to Ni and  $(\text{Au}, \text{Cu})_5\text{Sn}$  preferred to form next to Cu. When the reaction condition was 240°C for 2 min, the microstructure was the AuSn/ $\text{Au}_5\text{Sn}$ /Cu or AuSn/ $\text{Au}_5\text{Sn}$ /Ni layered structure.

The thermal stability of eutectic Au20Sn/Ni was better than that of Au20Sn/Cu when the samples were subjected to aging at 240°C. The Au20Sn/Ni could retain its microstructure at 240°C for more than 200 h, but that of Au20Sn/Cu changed in less than 10 h. Moreover, less Ni was consumed (0.8  $\mu\text{m}$ ) compared to that of Cu (4.8  $\mu\text{m}$ ) after 1000 h of aging. This indicates that Ni is a more effective diffusion barrier for the Au20Sn solder, and is a better surface finish from the perspective of being a more effective diffusion barrier.

### ACKNOWLEDGEMENT

This work was supported by the National Science Council of the Republic of China through Grant Nos. NSC-93-2216-E-008-001 and NSC-93-2214-E-008-002.

### REFERENCES

1. J.S. Pavio, *IEEE Trans. Electron. Dev.* 35, 1507 (1987).
2. G.S. Matijasevic and C.C. Lee, *Proc. 27th IEEE Int. Reliability Physics Symp.* (Piscataway, NJ: IEEE, 1989), pp. 137–140.
3. M. Nishiguchi, N. Goto, and H. Nishizawa, *IEEE Trans. Compon. Hybrid Manufacturing Technol.* 14, 523 (1991).
4. G.S. Natijasevic, C.Y. Wang, and C.C. Lee, *IEEE Trans. Compon. Hybrid Manufacturing Technol.* 13, 1128 (1990).
5. J. Ciulik and M.R. Notis, *J. Alloys Compounds* 191, 71 (1993).
6. J.Y. Tsai, C.W. Chang, Y.C. Shieh, Y.C. Hu, and C.R. Kao, *J. Electron. Mater.* 34, 182 (2005).
7. E. Zakel (Ph.D. Thesis, Technical University, Berlin, 1994).
8. B. Peplinski and E. Zakel, *Mater. Sci. Forum* 166, 443 (1994).
9. O. Karlsen, A. Kjekshus, and E. Rost, *Acta Chem. Scand.* 44, 197 (1990).
10. S. Anhöck, H. Oppermann, C. Kallmayer, R. Aschenbrenner, L. Thomas, and H. Reichl, *1998 IEEE/CPMT Berlin Int. Manufacturing Technology Symp. Proc.* (Piscataway, NJ; IEEE, 1998), pp. 156–165.
11. E. Zakel, G. Azdasht, and H. Reichl, *IEEE Trans. Compon. Hybrid Manufacturing Technol.* 4, 672 (1991).